Current Collection from the Space Plasma Through Defects in Solar Array Insulation

R. P. Stillwell,* R. S. Robinson,† and H. R. Kaufman‡
Colorado State University, Fort Collins, Colorado

Operating high-voltage solar arrays in the space environment can result in anomalously large currents being collected through small insulation defects. Tests simulating the electron collection have shown that there are two major collection modes. The first involves current enhancement by means of a surface phenomenon involving secondary electron emission from the surrounding insulator. In the second mode, the current collection is enhanced by vaporization and ionization of the insulator material, in addition to the surface enhancement of the first mode. The electron collection due to surface enhancement (first mode) has been modeled. Using this model, simple calculations yield realistic predictions.

Nomenclature

A = surface area of probe
A_a = area of annular ring
A_h = area of exposed conductor
b = constant dependent on trajectory of incoming electron
e = electronic charge
E = primary electron energy
E_m = primary electron energy at the value δ_m
I = electron current
J_0 = random current density
k = Boltzmann's constant
m_e = electronic mass
n = electron density
r_c = collection radius of insulator
T = temperature of sample
T_e = electron temperature
V = probe potential
V_a = potential of annular ring
V_c = conductor potential
V_{eff} = effective potential over collection region
α = constant dependent on radii of two spheres
β = material dependent absorption term
δ = secondary electron emission yield
δ_m = maximum value of secondary electron electron emission yield
ϵ_0 = permitivity of free space
θ = incident electron angle

Introduction

FOR spacecraft operation in the near-Earth environment, solar cell arrays constitute the major source of reliable long-term power. The minimization of total mass for such spacecraft results in the general requirement for high-voltage solar arrays. Exposed solar cells can collect large currents from the space plasma[1-4] with corresponding reductions in power output from the arrays. A protective covering of transparent insulation is not a complete solution to the current collection problem, due to the occurrence of defects, either from the manufacturing process or resulting from collisions with micrometeoroids.

Received Aug. 3, 1984, revision received Dec. 11, 1984.

*Graduate Student. Currently Member Technical Staff, TRW, Redondo Beach, CA. Member AIAA.
†Associate Professor, Department of Physics. Member AIAA.
‡Professor Emeritus, Department of Physics. Associate Fellow AIAA.

Early experiments by Cole, Ogawa, and Sellen[5] showed that positive electrodes behind a pinhole opening in the insulating sheet could collect electron currents as much as two orders of magnitude higher than predicted by electrostatic probe theory. They suggested that the electron collection could be explained by a secondary electron emission process. A subsequent investigation found that, for potentials up to 3000 V, polyimide (Kapton) insulation surrounding a pinhole collected a current only a factor of several magnitude greater than expected from electrostatic probe theory for high potentials.[6] At lower potentials, they found that the current collection was comparable to probe theory. In this investigation, Grier and McKinzie[6] postulated that the greater electron collection was due to sputtered insulation being ionized and thereby increasing the current collection.

A later paper by Grier and McKinzie[7] confirmed their previous results for other insulating materials, as well as reporting that the insulation around the holes appeared charred after testing. An investigation by Domitz and Grier[3] confirmed the results of Cole, et al.[5] that electron collection was orders of magnitude higher than expected. They further found that current collection was essentially independent of the hole size and of the electrode material behind the pinhole.

Results found by Kennerud[4] indicated that, for positive electrode potentials less than about 1000 V, the electron current was dependent on hole size. Above about 1000 V, the current became independent of hole size. Further reports of ground tests,[2,8,9] as well as space flight experiments,[10] continue to confirm that a small hole in an insulator collects orders of magnitude higher currents than could be expected from electrostatic probe theory.

Gabriel, Garner, and Kitamura[11] have probed the plasma sheath around a pinhole. They showed that the sheath is approximately hemispherical in geometry. However, analysis of the current collection indicates that the insulator did not contribute to the current collection and that their results can be explained with electrostatic probe theory.

Several computer simulations of electron collection have been made.[12-14] These simulations include the effect of secondary electron emission. Two of the simulations gave comparisons of electron collection with experimental results. The results of the computer codes were in rough agreement with data up to several hundred volts. The other simulation made predictions of the sheath potentials around the pinhole.[14] Unfortunately, the potential predictions cannot be verified. Although they were compared to Gabriel's data,[11] his data are of questionable validity in view of the fact that he observed current collection as comparable to probe theory.

From the observations above, previous investigations have reported contradictory results in the magnitude of the col-

lected currents and in the collection dependence of the hole size. Computer simulations of the collection have been unable to make accurate predictions for high potentials (>500 V). The present paper reports experimental results that reconcile the contradictory results. A model is also presented that describes the surface enhancement mechanism in the electron collection.

Apparatus and Procedure

Two vacuum facilities were used in the experiments. One was a 45 cm diameter, 72 cm long cylindrical glass vacuum system (the small vacuum facility). The other system was a 1.2 m diameter, 4.6 m long stainless steel vacuum system (the large vacuum facility) with a cryogenic liner. Some typical parameters for these systems are shown in Table 1. The plasma density range indicated in Table 1 approximates the environments expected for both an electrically propelled spacecraft, due to its own charge exchange plasma,[15] and a spacecraft in a natural low Earth orbit plasma environment.[1]

An argon hollow cathode was used to generate the plasma environment. A protected array of solar cells was simulated by placing a sheet of insulating material over a conductor. The insulating sheet was held to the conductor by a space-qualified adhesive, except for the few tests conducted to evaluate collection characteristics in the presence of lower-quality adhesives. A small hole was punched or drilled into the insulating sheet to simulate the defect. The adhesive holding the insulating sheet to the conductor was restricted to distances no more than 5 mm from the hole and, in most cases, extended up to the hole (hole punched through insulating sheet and adhesive simultaneously). Two sample designs were used, one with and one without control of the the sample temperature. The sample design with temperature control is shown in Fig. 1. The sample design without sample temperature control is a simplified version of that shown in Fig. 1.

The voltage sources were current and voltage regulated, 10,000 V, 100 mA direct-current power supply used for experiments in the large vacuum facility and a 150 kV, 5 mA direct-current unregulated power supply for tests in the small vacuum facility. Meters of appropriate ranges were used to measure the collected currents and the conductor potential.

The procedure for making a test was to allow the sample to be bombarded by the plasma (>30 min in the small system and >15 min in the large system) to desorb gases from the insulator surface. Bombardment by the plasma at longer times (several hours) did not make a difference in collection. The current collection through the hole was monitored as the potential on the conductor was increased. Sample temperatures were recorded and Langmuir probe measurements were taken to determine plasma properties before and after each test.

Experimental Results and Discussion

Collection Modes

Two distinct collection modes were observed for the positive-bias experiments. The two modes differed in electron collection by more than an order of magnitude. The first mode involved electron collection enhanced by a surface phenomenon (herein referred to as the surface-enhanced collection mode). This mode was characterized by a roughly linear current/voltage characteristic. It is speculated that the second mode involved vaporization of the insulator material (herein referred to as the vapor-enhanced collection mode). It appears that the vaporized material was ionized and thereby enhanced the electron collection. It has been observed in the large vacuum facility that, whenever there was a jump in the electron collection, the jump visually correlated with the appearance of a bluish glow located near the hole or a glow seen on the perimeter of the hole. The existence of two modes appears to explain some of the apparent contradictions in previous data.

The data for the surface-enhanced collection mode were taken only in the large vacuum facility where low background pressures were obtainable. The vapor-enhanced collection modes that are presented herein were taken in the small vacuum facility. The current/voltage characteristics taken in the small vacuum facility were typically of the shape shown in Fig. 2. In Fig. 2, the current/voltage characteristic begins with a very small current collection (not always seen with smaller holes), so the potential increases as the current increases until the mode changes occur. At this point, the potential drops and the current jumps. The potential drop was not seen when voltage regulation was used. Instead, the current would jump to a higher value at the same voltage. The upper region is the vapor-enhanced collection region. Operation in the latter region was usually accompanied by observation of a localized glow at the hole. The upper region where the current increases and conductor potential decreases represents the destruction of the insulator near the hole. An electron current high enough to cause rapid destruction was not always reached. After each test, the sample was always inspected. It was found that the insulator material was always discolored about the hole and a brownish layer of material deposited on the exposed conductor.

Normalization

During the experimental investigation, tests were performed in plasmas that varied in electron density by two orders of

Table 1 Typical parameters for the two vacuum facilities used in subject investigation

Parameter	Small vacuum facility	Large vacuum facility
Background pressure, Torr	$7-25\times10^{-5}$	$2-3\times10^{-5}$
Electron temperature, eV	4–9	4–13
Electron density, cm^{-3}	$2-10\times10^{5}$	$8-45\times10^{4}$

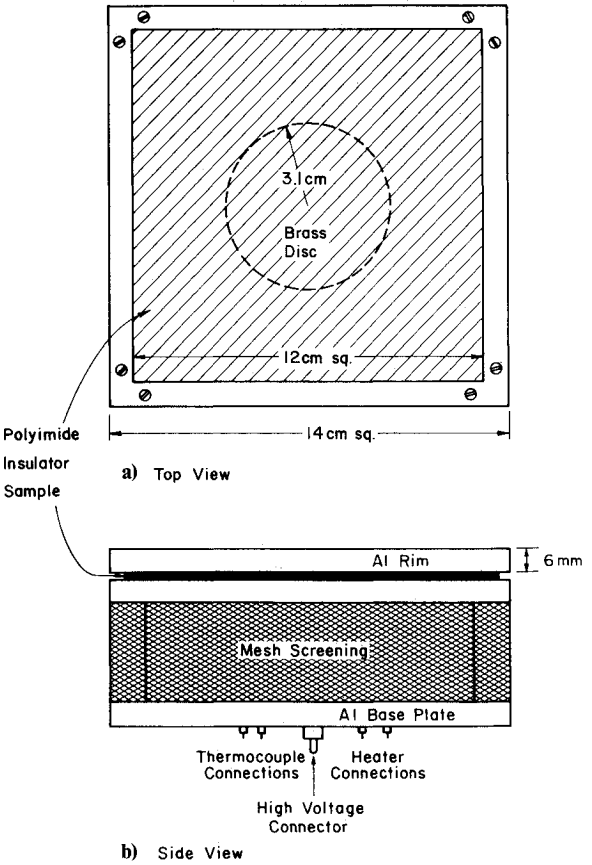

Fig. 1 Sample design heater.

magnitude and in electron temperature by a factor of several orders of magnitude. To effectively compare data taken under different plasma parameters, it was necessary to normalize the data.

To determine the correct normalization, the planar probe theory of Parker and Whipple[16] was examined. The current collection is given by

$$I = J_0 A\left[1 + \frac{b^2}{4} + \left(1 - \frac{b^2}{4}\right)\frac{eV}{kT_e}\right] \quad (1)$$

where J_0 is the random current density, given by

$$J_0 = \frac{1}{4} en\left[\frac{8kT_e}{\pi m_e}\right]^{1/2} \quad (2)$$

where n is the electron density, e the electronic charge, m_e the electronic mass, k the Boltzmann's constant, T_e the electron temperature, V the potential of the probe, and A the area of the probe. The constant b is adjustable ($0 \le b \le 2$) and is related to the incoming trajectories. From the form of Eq. (2), it can also be seen that b is a measure of the sheath, that is, for $b \to 0$ the sheath becomes detached from the collection area.

Sheath measurements have shown that the plasma sheath about a conductor surrounded by insulation has a roughly hemispherical shape.[4,11] The planar probe theory will have a hemisphere sheath for the condition $b \approx 0$. For this condition, the current collection is given by

$$I \simeq J_0 A \frac{eV}{kT_e} \text{ for } eV \gg kT_e \quad (3)$$

which has the same form as the current collection from spherical probe theory.[17] Equation (3) indicates that in analyzing the data, a normalized hole current, IkT_e/J_0, should facilitate comparison of data taken under different plasma conditions. A comparison of nonnormalized and normalized data is shown in Fig. 3 for the surface enhanced collection mode. Figure 3 clearly shows that, for the different plasma parameters, the current/voltage characteristics differ before normalization. But once the hole currents are normalized, the characteristics reduce essentially to one line. The straight lines through the data on Fig. 3 are least-square fits. In Fig. 3a, a slight jump in the current collection at 700 V occurs in one of the data sets. This jump was observed in many, but not all, of the data sets taken in the surface-enhanced collection mode. This jump should not be mistaken for the transition from the surface to the vapor-enhanced mode. The jump is small relative to the mode transition. The cause of this jump was not explored during this research.

In the vapor-enhanced collection mode, agreement between data taken under different conditions should be poor, since the vaporization and ionization of the vaporized material should be dependent on background pressure, roughness of hole, and surface history. Agreement after normalization was poorer than observed for the surface-enhanced collection mode.

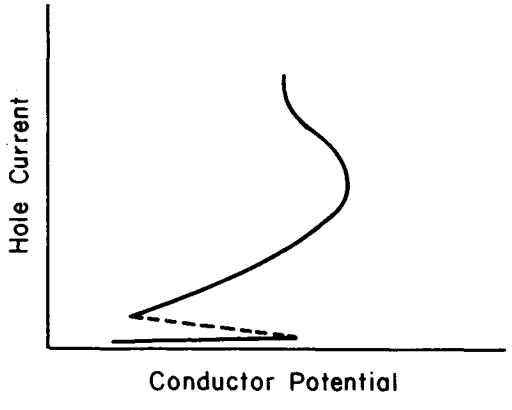

Fig. 2 Typical current-voltage characteristic observed in small vacuum facility.

Variation in Vapor-Enhanced Current Collection

While the data collected in the surface-enhanced collection mode were reproducible, those of the vapor-enhanced collection mode were far less so. This was especially true when comparisons were made of tests taken in the two different vacuum facilities. For electron densities and background pressures a factor of several magnitudes greater in the small vacuum facility, the normalized electron collection was also found to be greater by a factor of several magnitudes in that facility in the vapor-enhanced collection mode. This indicates that the magnitude of normalized current collection can differ significantly with plasma parameters and neutral density. This variation emphasizes that only rough agreement can be expected in the vapor-enhanced collection mode. The difference in electron collection was probably due to the variation in the amount of vaporization, caused by the difference in current density, and ionization, in turn caused by the difference in background pressure.

The data presented for the vapor-enhanced collection mode herein were all taken at the higher neutral pressures with electron densities in the range of 10^5-10^6 cm^{-3}.

Comparison with Electrostatic Probe Theory

In order to determine how the collected current is enhanced by the presence of the surrounding insulation, it is useful to make a comparison with electrostatic probe theory [Eq. (3)].

Figure 4 shows a comparison of the two collection modes with probe theory. The surface-enhanced collection mode

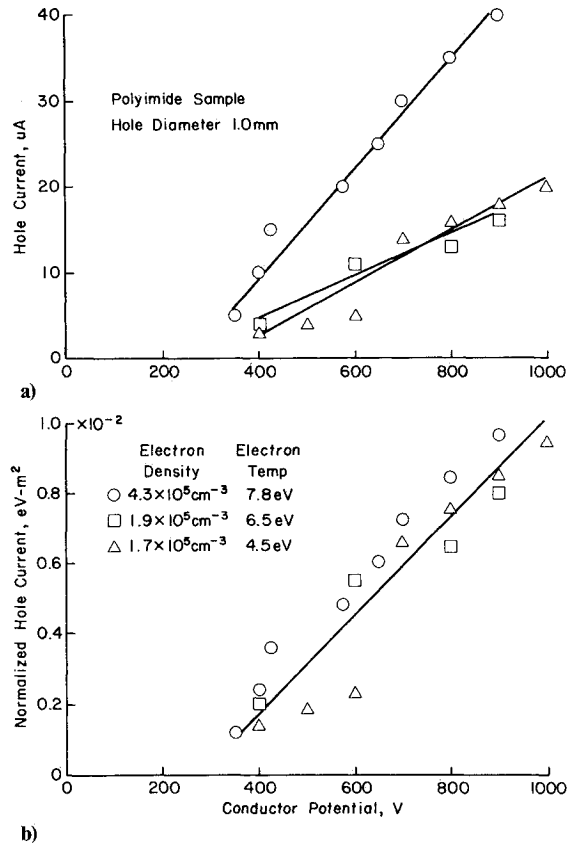

Fig. 3 Comparison of non-normalized and normalized current collection for the surface enhanced collection mode: a)non-normalized, b) normalized.

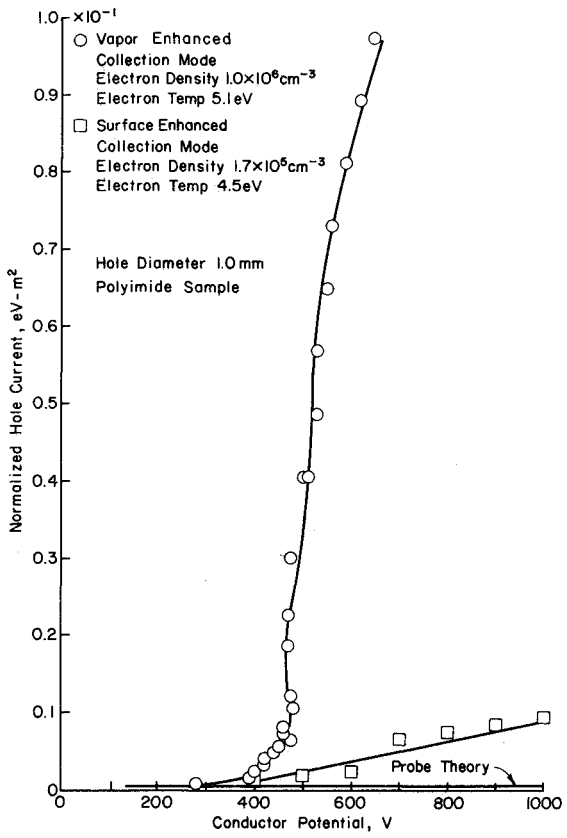

Fig. 4 Comparison of the two current collection modes with theory.

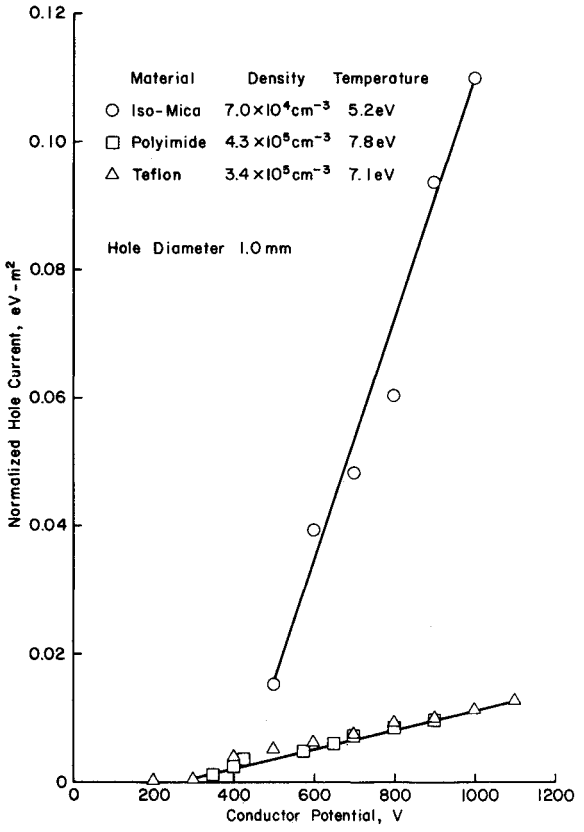

Fig. 5 Comparison of electron collection using polyimide, Teflon, and isomica insulators in the surface-enhanced collection mode.

gives electron currents approximately equal to probe theory at low voltages, up to an order of magnitude higher than probe theory at high voltages, while the vapor-enhanced mode yields currents over two orders of magnitude greater. This comparison illustrates the difference between the current collection that has been experimentally observed and what was theoretically predicted.

Adhesives

As described in the section on apparatus and procedure, the insulating material was held in contact with the conductor by an adhesive. Since the adhesive continued up to the hole edge, it was important to determine the effect of the adhesive on the electron collection.

Two types of double-sided pressure sensitive adhesives were tested, a low-priced commercial brand (Scotch Double Stick Tape, by 3M) and a space-qualified type (Y966, also by 3M). The low-priced commercial adhesive was found to have modified sticking properties after testing at high temperature ($<120°C$), while no such change was evident for the space-qualified adhesive. Such a change in properties for an organic material in a vacuum environment is almost always associated with outgassing. If the type of adhesive can affect the current collection, significantly different results should have been obtained with the two different adhesives tested.

The results of the adhesive tests in both collection modes showed no significant difference between the two adhesive types.

Sample Material

Three insulator materials were tested: polyimide, Teflon, and inorganically bonded isomica. The insulating materials were all thin sheets, the polyimide and Teflon 0.127 mm thick and the isomica 0.254 mm thick. All of the samples had hole diameters of 1.0 mm. The three materials were chosen because of widely different properties. In particular the secondary yield of the materials differ [18-20] and so different electron collection characteristics were expected.

Figure 5 compares the electron collection characteristics with the three insulator materials in the surface-enhanced collection mode.

Although Teflon and polyimide have different secondary yields, the current collection was found to be roughly equal. This will be discussed in the theory section.

Hole Size

Different hole diameters were tested to determine the effect of hole size on electron collection. For the surface-enhanced collection mode, five hole diameters were tested: 0.35, 1.0, 2.0, 3.0, and 5.0 mm. The results of these tests are shown in Fig. 6. It is indicated in Fig. 6 that the electron collection is strongly dependent on hole size in this collection mode. Analysis of the data shows that the current variation was less than proportional to the exposed conductor area, although the collected current increased continuously with increasing hole area.

Three different hole diameters were tested for the vapor-enhanced collection mode: 0.35, 1.0, and 2.0 mm. The results of these tests are shown in Fig. 7. The data of Fig. 7 show that the hole size is not important to the electron collection in this mode. This result is in agreement with the assumption that the vaporization and ionization of the insulating material is the dominant process in the vapor-enhanced collection mode.

The above results are also in agreement with the results found by Kennerud.[4] Although Kennerud did not recognize two collection modes, his data indicate that below a conductor potential of roughly 1000 V the current collection was dependent on hole size, but above this potential the current became independent of hole size. The data for the 2 mm hole diameter in Fig. 7 is an excellent example of the mode transition from the surface- to the vapor-enhanced collection mode. As can be observed from Fig. 7, the current collection is small until the transition occurs at approximately 625 V.

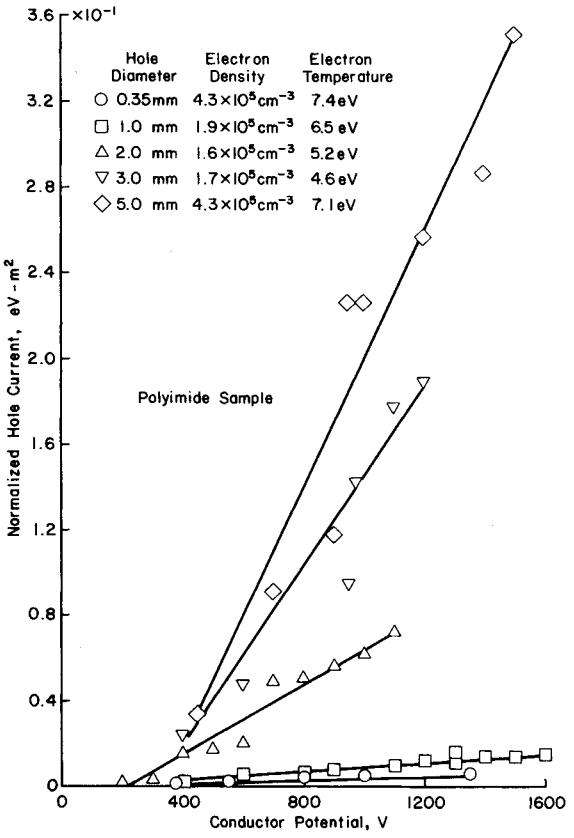

Fig. 6 Effect of hole size on current collection in the surface-enhanced collection mode.

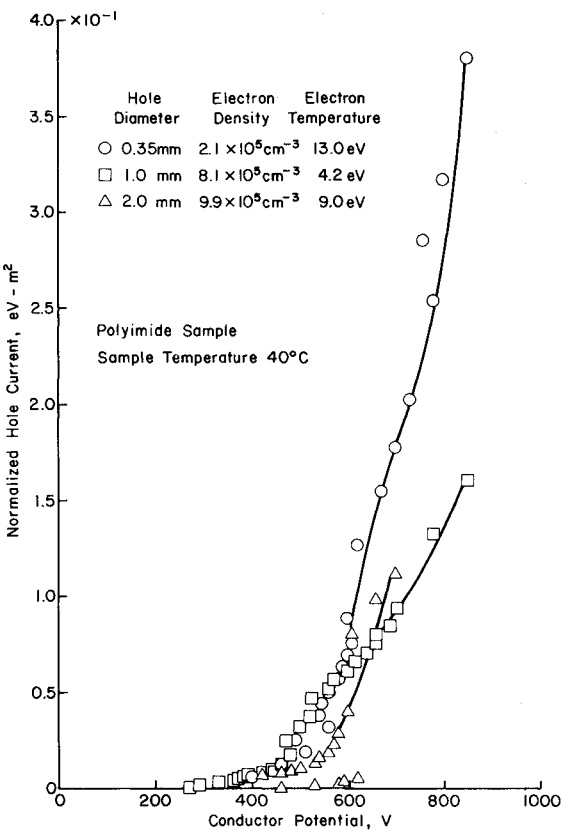

Fig. 7 Effect of hole size on current collection in the vapor-enhanced collection mode.

Textured Samples

To learn more about the surface phenomenon occurring, a textured sample was tested. The insulator surface was textured by mechanically rubbing a fine grade of sandpaper over the surface facing the plasma. This was done before cleaning and punching the hole in the sample. The results of this test showed a 20-60% decrease in electron collection for the textured sample in the surface-enhanced collection mode. The amount of current decrease was roughly constant from 500 to 2400 V, so that it was a smaller percentage at higher voltages.

It has been found that roughening a surface decreases the secondary electron emission yield.[21] The collection mechanism suggested by Cole et al.[5] could therefore explain this observation.

To determine if a surface phenomenon plays any part in the vapor-enhanced collection mode, textured surfaces were also tested in this mode. The samples were textured in a different manner for these tests. Radial lines and concentric circles were scribed onto the surface, radiating from the hole, with a sharp metal stylus. The results of these tests showed a decrease of 75%, or more, in the electron collection by a textured sample. This indicated that some of the same surface phenomena observed in the surface-enhanced mode are still operating and important to the collection process in the vapor-enhanced mode.

Sample Temperature

The temperature of the sample was varied to determine the effect of this variable. It was found that increasing the temperatures caused decreased electron collection for polyimide in both collection modes. This is consistent with results obtained by a Soviet investigator[18] who found that decreasing secondary yields results from increasing temperatures for polymers.

In the vapor-enhanced collection mode, the increasing temperature might have been expected to increase collection by increasing vaporization. On the other hand, secondary emission often decreases with increasing temperature.

To determine if secondary emission is responsible for the current decrease with increasing temperature, a mica sample was also tested. This insulator selection was made because it has been found that mica does not have a significant temperature dependence for secondary yield.[19]

The isomica sample was tested six times at three different temperatures: 27, 50, and 85°C (two tests per temperature). The results indicate that electron collection is independent of sample temperature. This also indicates that the spread observed with polyimide was indeed due to secondary electron effects.

A polyimide sample with a 5.0 mm hole diameter was tested. It was found that, for this hole diameter, there was no appreciable temperature effect. As the hole size is increased, a larger fraction of the electron current would be expected to be collected directly by the exposed conductor. This would have the effect of reducing any temperature effect by decreasing the fraction of the total electron current that strikes the surrounding insulator material.

Onset of Vaporization

In discussing the two types of collection modes, the conditions necessary for a mode change have been ignored. This section will discuss the observation made on the transition from one mode to another.

The probable mechanism for the mode change is as follows. The electron collection increases (in the surface enhanced mode) to a level where the current density flowing into the hole is sufficient to vaporize the insulator by joule heating. At this point, the current collection enters the vapor-enhanced collection mode. The mode change was seen to occur at lower potentials in the small vacuum facility. This observation is believed to be due to the higher electron densities hence the higher collection in this facility.

As defined here, the onset of vaporization is the point at which the current collection deviated from the expected normalized data for the 1.0 mm diameter hole. In the case of the other hole sizes, the onset was defined as either the point at which the current departed significantly from a linear extrapolation from lower-voltage data or the point at which the current jumped to a higher value.

When current jump was observed, it was accompanied by a bluish glow localized about the hole or a glow on the perimeter of the hole. These visual observations are consistent with the insulator material being vaporized. The vaporized material would enhance the local neutral density about the hole so that the ionization of this material would increase both the local plasma density and current collection.

For different hole sizes, it was found that the trend was for larger holes (above 2 mm) to require more power before vaporization occurred, as shown in Fig. 8. The scatter shown in Fig. 8 for the 1.0 mm diameter hole was probably due to variation in the roughness of the hole edge. A large number of tests were made with this hole diameter and, if the hole edge was rough, this would allow some vaporization to occur at low power levels. If more tests had been conducted at the other hole diameters, similar scatter might have been observed elsewhere in Fig. 8.

Comparison of data for different sample temperatures results in a rough trend of reduced power required for the onset of vaporization with increasing temperature. However, the data were not sufficiently complete to support this conclusion with a high degree of confidence.

Subsequent Tests after Vaporization

It was found that once vaporization had occurred, the results of that test could not be repeated on the same sample. Subsequent tests on the same sample showed a substantial decrease in electron collection, frequently by a factor of 10 or more. One possible explanation was that the effect was due to adsorbed gas layers on the insulator surface. As time passes, the electron bombardment of the insulator removes the adsorbed layers, changing the surface properties. This possibility was tested by using a fresh sample, then removing it from the small vacuum facility after testing, and exposing it to air for 17 hours. The sample was then replaced and tested again. The second testing showed drastically reduced current collection from the first test, indicating that removal of adsorbed gas layers was not the cause of the current reduction.

Another possiblity was that, when the vaporized material deposited the brownish film over the exposed conductor, the presence of this film reduced electron collection. This possibility was tested by constructing a sample holder that allowed the conducting disk beneath the insulating sheet to be rotated to a clean portion of the copper. These tests showed that the current collection still decreased with subsequent tests.

The only other likely possibility appeared to be that, once vaporization of the insulator material occurs, it changes the secondary electron emission yield of the material. In this regard, tests on the mica sample are of interest. In those tests, the same sample was used successively six times without a noticeable decrease in electron current, when tested in the surface-enhanced collection mode. Mica is more resistant, in general, to thermal and electrical damage than most materials, so that greater resistance to such damage might be expected.

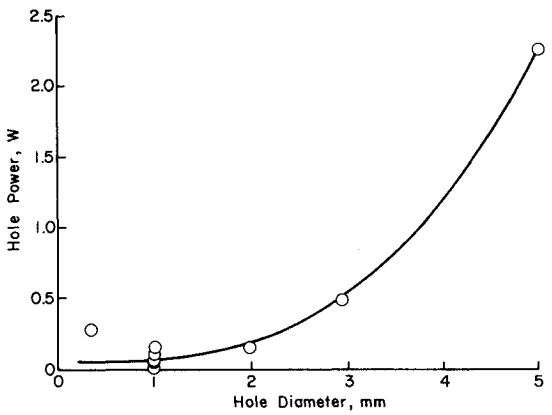

Fig. 8 Power required for the onset of vapor-enhanced mode for a polyimide sample is hole diameter.

Healing Effect

Occasionally during a test in the vapor-enhanced collection mode, the current began to drop. This "healing" only occurred in this mode. No correlation can be found between the power at the point of current decrease and background pressure on plasma conditions (see Table 2)

The probable cause of the healing is vaporized material being deposited on the conductor to an extent sufficient to reduce electron collection. Kennerud[4] reported similar behavior for Teflon, indicating that this behavior may be common to many types of insulators.

Theory

The electron collection model presented herein is similar to that proposed in a qualitative manner by Cole et al.[5] and is intended to represent only the surface-enhanced collection mode. An incoming electron strikes the insulator surface near the hole, emitting a secondary electron. The secondary electron is then attracted toward the exposed conductor by a potential gradient. In this manner, an incoming electron striking the insulator close to the hole causes an electron to be collected by the exposed conductor.

Plasma Sheath

As previously mentioned, sheath measurements have shown that the sheath about the pinhole is roughly hemispherical in shape. A remaining question then is whether the electron collection through the sheath is space charged or orbit limited.

To determine if the electron flow were space charge limited, currents were calculated for space charge flow between two concentric spheres. The hole radius was used as the radius of the inner sphere and an empirially determined sheath radius was used for the outer sphere radius. This sheath radius was found by determining the sheath size needed to collect the observed current from the plasma. The current collection for space charge flow is given by[22]

$$I = 16\pi\epsilon_0 \frac{\sqrt{2}}{9}\sqrt{\frac{e}{m_e}}\frac{V^{3/2}}{\alpha^2} \tag{4}$$

where ϵ_0 is the permitivity of free space, e the electronic change, m_e the electronic mass, and V the potential difference between the spheres. α is a term that is dependent on the ratio of the radii of the two spheres. These calculations showed that the currents expected from space charge flow were more than

Table 2 Conditions for current decrease in vaporization-enhanced collection mode for a 1.0 mm diameter hole in polyimide at 27°C.[a]

Power, W	Electron density, cm^{-3}	Electron temperature, eV	Neutral pressure, Torr
0.36	4.3×10^5	7.8	2×10^{-5}
0.23	2.0×10^5	6.0	1.9×10^{-5}
0.13	1.5×10^5	8.1	2×10^{-5}
0.13	1.9×10^5	9.9	2×10^{-5}
0.10	1.7×10^5	10.9	2×10^{-5}
0.09	2.3×10^5	12.8	2×10^{-5}

[a] All data taken in large vacuum facility.

two orders of magnitude larger than the observed currents for the surface-enhanced collection mode.

The space charge-limited flow calculations thus demonstrated that the current collection was orbit limited. that is, not all electrons that entered the plasma sheath were collected. The approach to modeling should therefore be to modify an orbit-limited theory to include part of the insulator as a collector. The most likely theory to start with is the planar probe theory of Parker and Whipple.[16] The planar probe theory has the correct geometry as well as an approximately hemispherical sheath. The collected current is given by Eq. (3).

Collection Area

Two approaches to the collection area were tried. The first approach used the assumption that the entire surface area under the plasma sheath contributed to electron collection. Trajectories for the secondary electrons moving across the insulator surface were calculated. As might be expected, for a radial electric field, all of the secondary electrons produced struck the exposed conductor. For polyimide and conductor potentials between 50 and 1000 V, the insulator charged to potentials greater than the conductor potential, inasmuch as the secondary yield was greater than one in this range. For an insulator surface with a potential greater than the conductor potential, a potential gradient would be formed that would repel electrons from the hole, except for those secondaries produced at the hole edge. This approach did not appear promising.

In the second approach, only a small annular ring of insulator near the hole contributed to the electron collection. For simplicity, it was assumed that this annular ring was at a constant potential. This assumes that the potential gradient is slight over the majority of the insulator contributing to collection and that the potential gradient is concentrated at the edge of the collection area. In this approach, the condition for continuity of charge is given by

$$(A_a + A_h)/A_h = \delta \tag{5}$$

where A_a is the area of the annular ring, A_h the area of the exposed conductor, and δ the secondary electron emission yield (see Appendix A). The implicit assumption in Eq. (5) is that the fraction of the secondary yield that is collected by the conductor is proportional to the fraction of hole area divided by total collection area $(A_a + A_h)$.

To demonstrate that Eq. (5) is a condition for continuity of charge, consider a secondary electron yield of four. From Eq. (5), the annular ring area is three times that of the hole area; consequently, an incoming electron striking within the collection radius r_c causes four secondary electrons to be emitted. Of the four electrons, three again strike within the annular ring and one is collected by the conductor. In this manner, one electron is collected by the conductor for each electron striking the insulator and the charge on the annular ring is maintained constant during steady-state conditions. Also note that the energy of a secondary is, in general, too small to produce tertiary electrons.

Using Eq. (5) as a basis for a model, the planar probe theory can easily be modified. The probe potential in Eq. (3) should be an effective potential over the collection region. The value used was the average potential over the collection area, that is

$$V_{\text{eff}} = \frac{V_c A_h + V_a A_a}{A_h + A_a} \tag{6}$$

where V_c is the conductor potential and V_a the potential of the annular ring.

This model was compared to experimental data to determine if it had any physically realistic solutions. The data used in this comparison were for a 1.0 mm diameter hole with an electron density of 1.6×10^5 cm^{-3} and electron temperature of 4.5 eV. The calculation procedure used for a given collector voltage V_c was as follows:

1) Pick a value of r_c (collection radius of insulator).

2) Calculate V_{eff} from probe theory to match the experimentally observed current [i.e., $V_{\text{eff}} = IkT_e/J_0(A_h + A_a)$].

3) Calculate V_a needed for the assumed values V_{eff} and r_c, *i.e.*, $V_a = [(A_h + A_a)V_{\text{eff}} - V_c A_h]/A_a$.

4) Calculate δ from the value of V_a (see Appendix A).

5) Repeat above steps for different values of r_c and plot the physical values of V_a (i.e., $V_a \leq V_c$) against the corresponding values of δ from step (4). These results are compared with values from the expression for δ.

The results of this procedure are shown in Fig. 9, where the possible physical solutions for this model are shown to vary over a range of mean incidence angle. The data used in Fig. 9 are from those shown in Fig. 3 for $T_e = 4.5$ eV. The results of the calculation procedure are indicated by the lines with different assumed values of V_a, while the permissible values of secondary electron emission are indicated by the incident angles (≤ 90 deg).

The gap in the permissible solutions between 600 and 700 V is the result of a slight current collection increase. But as demonstrated in Figs. 3 and 4, there is only a small deviation from linear current collection.

Model

The next task in formulating the model is to determine an effective angle for the incoming electrons to strike the insulator. Since the flow is orbit limited, the path of the electron is not radial. With this in mind, a reasonable approximation for the angle is the value that gives the same secondary electron emission as the average of the angular dependence term of the secondary yield over the surface of a hemispherical sheath. This is given by

$$\langle e^{\beta E^{1/2}(1-\cos\theta)} \rangle = \int_0^{2\pi} d\psi \int_0^{\pi/2} e^{\beta E^{1/2}(1-\cos\theta)} \sin\theta d\theta \div \int_0^{2\pi} d\psi \int_0^{\pi/2} \sin\theta d\theta = 1/\beta E^{1/2} \{ e^{\beta E^{1/2}} - 1 \} \tag{7}$$

Over a range of 1400 eV, the angle corresponding to an averaged angular dependence of δ varied at 65 to 72 deg, increasing with increasing energy. The calculations presented in Fig. 9 indicate that solutions with angles in this range require annular ring potentials close to the conductor potential. There is, therefore, little loss of accuracy in assuming the potential of the annular ring is the same as the conductor potential.

Having determined the potential and incident angle requirements on the annular insulator ring, the model can be used to predict electron collection for the surface-enhanced collection mode. The procedure for predicting current collection is shown in Appendix B.

From the model as presented, the collection radius is a critical parameter in determining the collected current. The collection radius is shown in Fig. 10 as a function of conductor potential for three hole diameters, 1.0, 3.0, and 5.0 mm. The calculations shown in Fig. 10 indicate that, after an initial sharp increase, the collection radius increases more slowly with increasing conductor potential. This behavior leads to current/voltage characteristics that are roughly linear for high conductor potentials.

Comparison with Experimental Data

To determine how well the model predicts the current/voltage characteristics, the model can be compared to experimental data. The comparisons are shown in plots of normalized hole current IkT_e/J_o vs conductor potential.

The calculated current collection is compared to the experimetal data in Fig. 11 for a 1.0 mm diameter hole at three

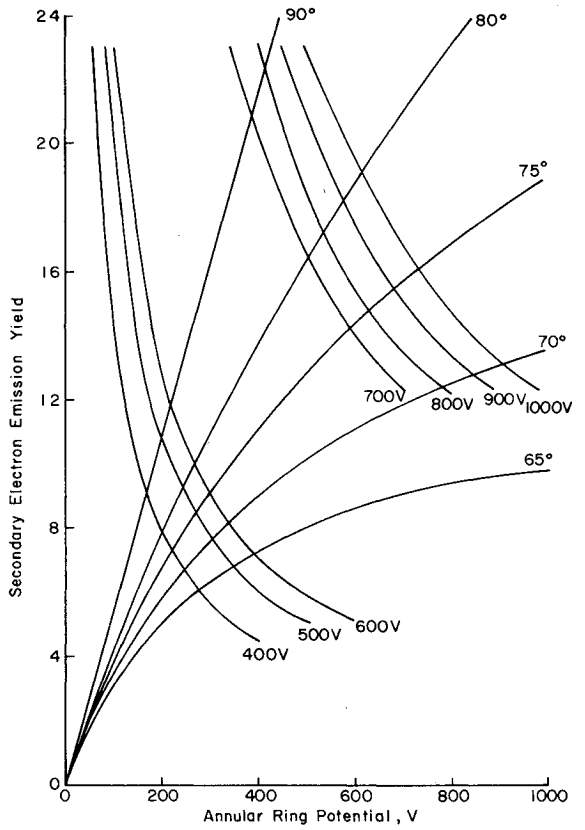

Fig. 9 Range of possible solutions for an experimental data set.

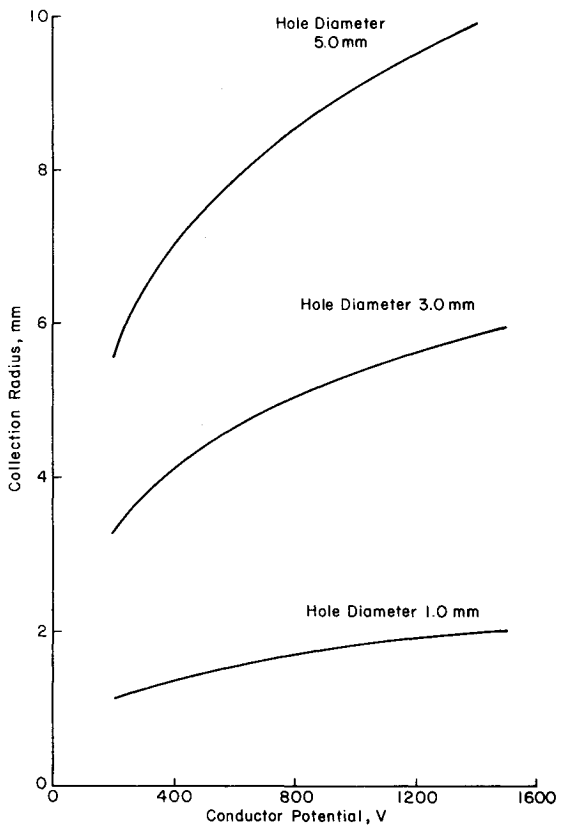

Fig. 10 Collection radius as a function of conductor potential and hole diameter.

different plasma conditions. The predicted and experimental values are in excellent agreement.

Hole Size

The model is compared to experimental data for three different hole diameters (1.0, 3.0, and 5.0 mm) in Fig. 12. The model predicts the effect of hole size quite well, with experiment and theory agreeing within a factor of two.

Sample Temperature

It was found that, for a 1.0 mm diameter hole in polyimide, increasing sample temperature resulted in a decrease in current collection. A comparison of the theory with experiment (see Fig. 13) shows that the model also predicts a decrease in current with increasing sample temperature, but not of the magnitude the data indicate. This will be discussed later in this paper.

In testing a 5.0 mm diameter hole in polyimide, no sample temperature effect was observed. However, the model still predicts a temperature effect. In fact, the temperature effect is proportionally the same as for the 1.0 mm diameter hole. That is, for a similar temperature increase, the predicted current drops by the same ratio. This disagreement with observed behavior cannot be explained at this time.

While testing isomica, it was found that there was no sample temperature effect. The literature reports that the secondary yield for mica is temperature independent.[19] From Eq. (5), it can be readily seen that the theory predicts no temperature effect if the secondary yield is independent of temperature. The absence of a temperature effect is thus correctly predicted for mica.

In demonstrating that increasing sample temperature decreases current collection for polyimide, it has been shown that any parameter that decreases the secondary yield also decreases electron collection. This was illustrated in the observed effect of sample roughness. Roughening a surface decreases the secondary yield[21] and, as such, the model predicts that the current collection should decrease. This is in agreement with observed experimental data.

Insulator Material

Two sample materials (polyimide and Teflon), whose secondary yields are known, were tested. On first inspection, their secondary electron emission yields appear sufficiently different to cause different electron collection (the primary reason for choosing the two materials). After testing, when the averaged angular dependence [Eq. (7)] was selected for the secondary yield, the coefficients were found to be very similar. This similarity in the average secondary yield explains why two apparently dissimilar materials produced very similar electron collection (see Fig. 14).

For data on the secondary yield for mica show that the yield varies for different types of mica. Since the yield for the mica tested was unknown, the model was not applied to the mica sample. However, the mica samples did indicate that the secondary yield appears to be higher for mica than for polyimide and Teflon.

Discussion of the Model

There is no comprehensive theory for secondary electron emission. Therefore, it is necessary to rely to a large extent on experimental data. Unfortunately, the data on polymers are quite limited. Some studies were carried out from the late 1950s in the USSR. It is only recently (early 1970s) that such studies were started in the United States. Furthermore, only one study (to the authors' knowledge) has been made on the temperature and angular dependence of polymers in the energy regime of interest here and that study did not include polyimide.

From these observations, the reader should be aware that the accuracy of the model is dependent on the accuracy of the secondary electron emission yield. This is particularly true with regard to the temperature dependence of the model. One

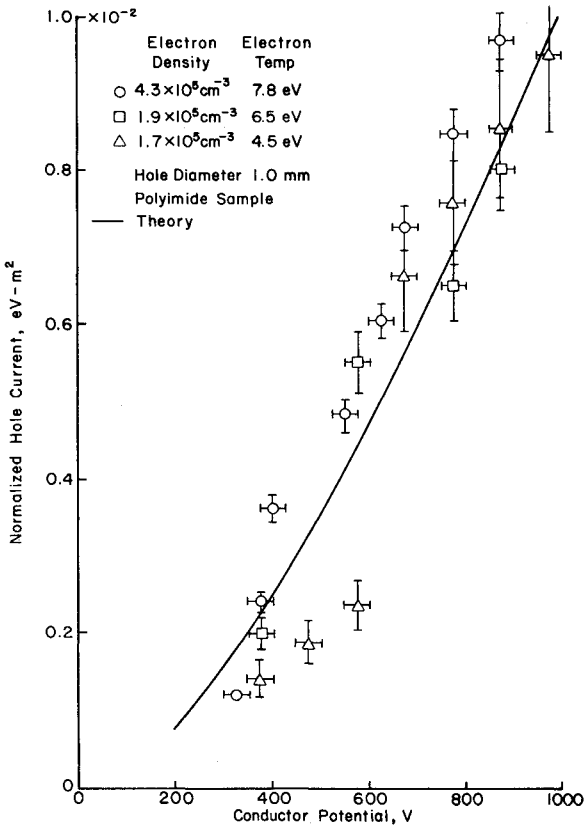

Fig. 11 Comparison of theory and experiment for different plasma conditions.

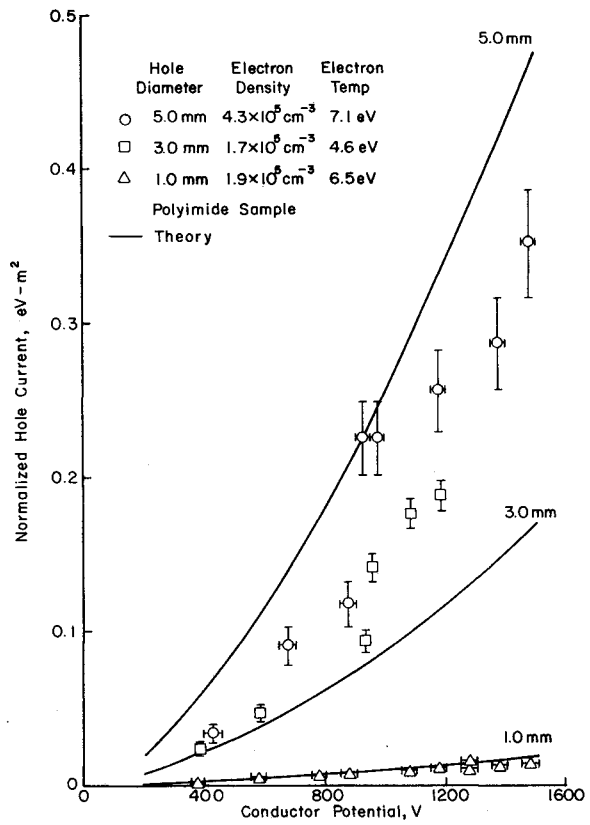

Fig. 12 Comparison of theory and experiment for different hole diameters.

secondary emission theory that is used herein predicts a temperature dependence that increases with energy and angle, although the experimental evidence generally does not support this. On the other hand, the temperature dependence used in the model comes from a different theory[23] and is generally supported by experiment. The contradiction can be illustrated with the one experimental study done on the temperature effect for a polymer[18] (polystrene). In this study, it was found that the temperature dependence differed from Dekker's theory[23] and was somewhat dependent on angle. This result indicates that the temperature dependence of the secondary yield for polymers must be considered questionable and that more studies need to be done before the temperature dependence can be defined.

The assumption was made that the electrons arrived at the surface with an equal probability from all solid angles within the permissible hemisphere. This assumption appears reasonable, but since the electron flow is orbit limited, an argument can be made that the electrons should strike more frequently at grazing angles. If the mean effective angle was increased by 10%, the predicted current would be higher. It would, for example, still be within a factor of two of the presently predicted currents over the conductor potential range of 200-1500 V for a 1.0 mm diameter hole. As indicated by this example, the assumption of angular distribution for electrons is believed to result in at least qualitatively correct predictions.

It was also assumed that the exposed conductor collects secondary electrons proportional to its fraction of the total collection area. If, because of electric fields, the exposed conductor collected twice the number of secondary electrons indicated by exposed area, the collection radius would be reduced. The predicted currents would then be 6-20% lower than presently predicted values for a 1.0 mm diameter hole in polyimide and a conductor potential of 200-1500 V. The possi-

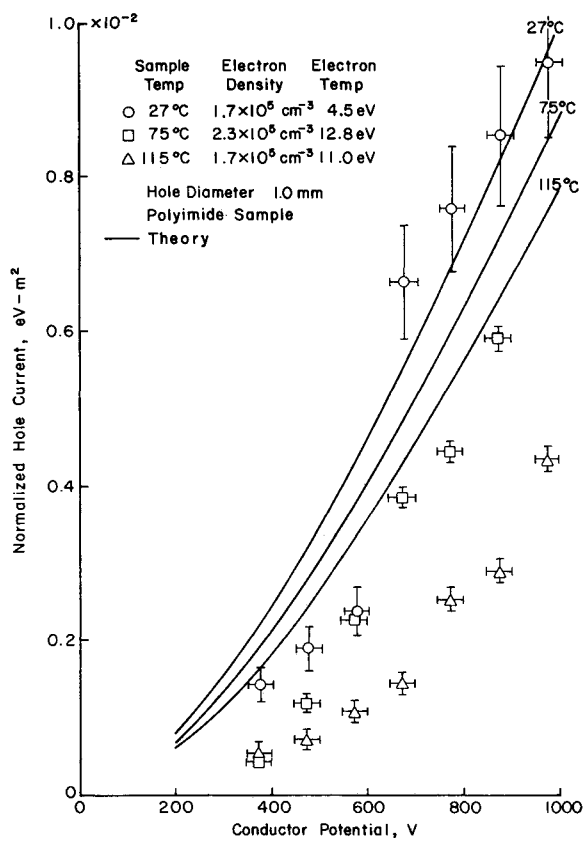

Fig. 13 Comparison of theory and experiment for different sample temperatures.

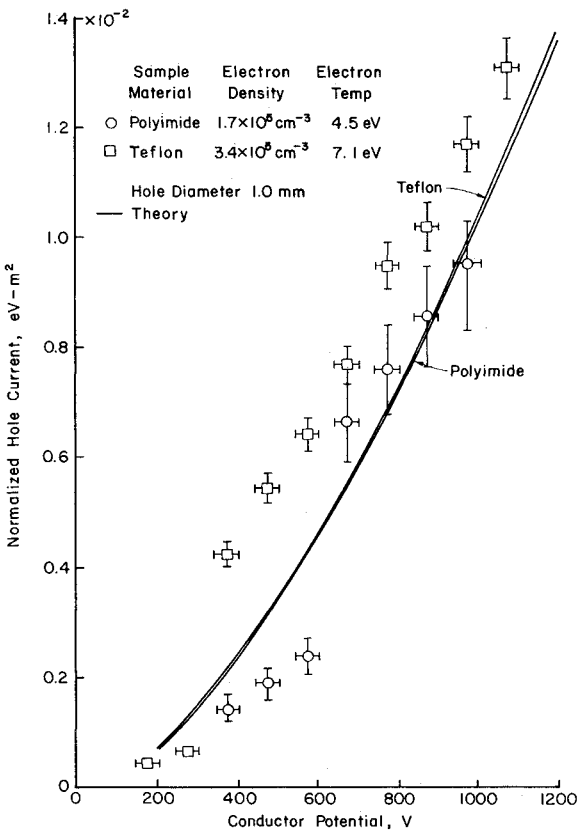

Fig. 14 Comparison of theory and experiment for different insulator materials.

ble adverse effects of this area-proportional collection assumption are therefore believed to be small.

Conclusion

This investigation has identified two electron collection modes. One mode involves only the surface of the surrounding insulator, thereby enhancing the current collection. The second mode involves the same surface enhancement plus an additional enhancement due to the vaporization and ionization of the surrounding insulator. The occurrence of the second mode depends on the enhanced current collection of the first mode.

The surface enhancement has been found to be a function of the secondary electron emission yield of the surrounding insulator. As such, parameters that decrease the secondary yield also decrease electron collection.

The vapor-enhanced collection mode exhibits all the same properties as the surface-enhanced mode except the dependence on hole size. It was found that the electron collection in this mode appears to be essentially independent of this hole size up to 2.0 mm. The results of this investigation show that more work is necessary for the vapor/enhanced collection mode. This work should attempt to further define the point at which the mode change occurs.

A model for the surface-enhanced collection mode has been presented. In the model, a self-consistent description of the role of secondary electron emission is given. Using this model, simple calculations yield realistic predictions that include all the major features found in experimental investigations. The predicted current collection is generally within a factor of two of experimental values at the same conditions. The model depends strongly on knowledge of the secondary electron yield and, as such, is sensitive to uncertainties in this knowledge.

Table A1 Important parameters in the secondary electron emission yields for polyimide[24] and Teflon[20]

Parameter	Polyimide	Teflon
δ_m	1.8	235
E_m, eV	250	410
β, eV^{-1}	0.126	9.88×10^{-2}

Appendix A: Secondary Electron Emission

The form of the secondary electron yield is given by [24]

$$\delta(E,\theta)=e^{\beta E^{1/2}(1-\cos\theta)}\delta m\frac{E}{E_m}e^2e^{-\beta E^{1/2}} \tag{A1}$$

where E is the primary electron energy, θ the incident electron angle (measured from the surface normal), δ_m the maximum value of the secondary yield, E_m the primary energy at the value δ_m, and β a material-dependent absorption term. β is related to E_m by the expression

$$\beta=2/E_m{}^{1/2} \tag{A2}$$

Table A1 shows the various values for secondary emission for two materials (polyimide and Teflon).

The temperature dependence of the secondary yield used in the model is given by the relation[23]

$$\frac{\delta(T_1)}{\delta(T_2)}=\frac{T_2}{T_1} \tag{A3}$$

were T is the temperature. Although data from polymers[18] indicates that the secondary yield does not follow a $1/T$ temperature dependence, Eq. (A3) does have the secondary yield decrease with increasing temperature. The relation given by Eq. (A3) will be used for the lack of any better expression.

Appendix B: Procedure for Calculating the Electron Collection from the Model

1) Calculate the effective incident angular dependence for the secondary emission yield at a given conductor potential [Eq. (7)].

2) Calculate the secondary yield from the conductor potential using this angular dependence and

$$\delta(E)=<e^{\beta E^{1/2}(1-\cos\theta)}>\delta_m\frac{E}{E_m}e^2e^{-\beta E^{1/2}}$$

3) Calculate the annular ring area from Eq. (5).

4) Calculate the electron current for the given plasma conditions using

$$I\simeq J_0(A_h+A_a)\frac{eV}{kT_e}$$

from planar probe theory.

Acknowledgment

This work was supported by NASA Grant NSG-3196.

References

[1]White, R. S., *Space Physics*, Gordon and Breach, Science Publishers, Inc., New York, 1970.

[2]Bayless, J. R., Herron, B. G., and Worden, J. D., "High Voltage Solar Array Technology," *Journal of Spacecraft and Rockets*, 1973, pp. 457-462.

[3]Domitz, S. and Grier, N. T., "The Interaction of Spacecraft High Voltage Power Systems with the Space Plasm Environment," NASA TMS-71554, June 1974.

[4]Kennerud, K. L., "High Voltage Solar Array Experiments," NASA CR-121280, March 1984.

[5]Cole, R. K., Ogawa, H. S., and Sellen, J. M., Jr., "Operation of Solar Cell Arrays in Dilute Streaming Plasmas," AIAA Paper 69-262, March 1969.

[6]Grier, N. T. and McKinzie, D. J. Jr., "Current Drainage to a High Voltage Probe in a Dilute Plasma," NASA TMS-67890, Dec. 1972.

[7]Grier, N. T. and McKinzie, D. J. Jr., "Measured Current Drainage through Holes in Various Dielectrics up to 2 Kilovolts in Dilute Plasma, NASA TND-6663, Feb. 1972.

[8]Grier, N. T., "Experimental Results on Plasma Interactions with Large Surfaces at High Voltages," NASA TM-81423, Jan. 1980.

[9]Stevens, N. J., Berkopec, F. D., and Purvis, C. K., "Investigation of High Voltage Spacecraft Systems Interaction with Plasma Environments," NASA TM-78831, April 1978.

[10]Grier, N. T. and Stevens, N. J., "Plasma Interaction Experiments (PIX) Flight Results," NASA CP-2071, 1978, pp. 295-314.

[11]Gabriel, S. B., Garner, C. E., and Kitamura, S., "Experimental Measurements of the Plasma Sheath around Pinhole Defects in a Simulated High Voltage Solar Array," AIAA Paper 83-11, Jan. 1983.

[12]Chaky, R. C., Nonnast, J. H., and Enoch, J., "A Numerical Simulation of Plasma-Insulator Interactions in the Spacecraft Environment," *Journal of Applied Physics,* Vol. 53, 1981, pp. 7092-7098.

[13]Mandell, M. J., Datz, I., and Cooke, D. L., "Potentials on Large Spacecraft in LEO," *IEEE Transactions on Nuclear Science,* Vol. NS-29, 1982, pp. 1584-1588.

[14]Mandell, M. J. and Katz, I., "Potentials in a Plasma Over a Biased Pinhole," *IEEE Transactions on Nuclear Science,* Vol. NS-30, 1983, pp. 4307-4310.

[15]Kaufman, H. R. and Isaacson, G. C., "The Interactions of Solar Arrays with Electric Thrusters," AIAA Paper 76-1051, Nov. 1976.

[16]Parker, L. W. and Whipple, E. C., "Theory of a Satellite Electrostatic Probe," *Annals of Physics,* Vol. 44, 1967, pp. 126-167.

[17]Chen, F. F., "Electric Probes," *Plasma Diagnostic Techniques,* edited by R. H Huddlestone, and S. L. Leonard, Academic Press, New York, 1965.

[18]Matshevich, T. L., "Secondary Electron Emission of Some Polymers," *Fizika Tverdogo Tela,* Akademiya Nauk SSSR, Vol. 1, 1959 pp. 277-281 (in Russian).

[19]Fridrikhov, S. A. and Shulman, A. R., "An Investigation of the Secondary Electron Emission by Certain Dielectrics at Low Primary Electron Energies," *Soviet Physics—Solid State,* Vol. 1, 1960, pp. 1153-1159.

[20]Leung, M. S., Tueling, M. B., and Schnauss, E. R., "Effects of Secondary Electron Emission on Charging," *Spacecraft Charging Technology Conference,* NASA CP-2182, 1980.

[21]Rashkovskii, S. F., "Secondary Emission from Rough Surfaces," *Radio Engineering and Electronic Physics (USSR),* Vol. 3, 1958.

[22]Langmuir, I. and Blodegett, K. B., "Currents Limited by Space Charge Between Concentric Spheres," *Physical Review,* Vol. 23, 1924.

[23]Dekker, A. J., "On the Escape Mechanism of Secondary Electrons from Insulators," *Physica,* Vol. 21, 1955, pp. 29-38.

[24]Sternglass, E. J., "On the Phenomenon of Secondary Electron Emission from Solids," M. S. Thesis, Cornell University, Ithaca, N.Y., 1951.